RESEARCH ARTICLE

Editorial Process: Submission:02/26/2025 Acceptance:02/27/2026 Published:03/06/2026

Bone Cancer Cell Prediction Using an Enhanced Deep Learning Algorithm with an Optimization Technique

Mohanthi Kakarla[1]*, K Padma Raju[2]

Abstract

Objective: Bone cancer is a very serious disorder that can be fatal for many people. A reliable detection and classification system is required for early-stage bone cancer diagnosis. Traditional manual approaches are time-consuming and need specific skills, thus the creation of an automated system for detecting and classifying malignant and healthy bone tissue is critical. Cancerous bone tissue often has a different texture than healthy tissue in the affected location. Despite initially using Support Vector Machine and Edge Detection methods to improve outcomes, we only reached 0.92% accuracy. As a result, moving to deep learning is important for improved performance. Our strategy will begin with feature extraction, followed by the usage of the Cuckoo Search optimization algorithm. **Methods:** The methodology emphasizes rigorous data preprocessing, model evaluation using standard metrics, and clinical integration for real-world application. It aims to develop a machine learning (ML)-driven tool for bone cancer detection by utilizing a combination of deep learning (DL) models and optimization methods. It includes enhancing detection accuracy by integrating Cuckoo Search Modified Hill Climbing (CS-MHC) optimization with ResNet for improved image classification, optimizing model performance through CSO for better feature selection and faster convergence, comparing the CS-MHC ResNet model with traditional models like VGG-16, Inception, and Xception to improve accuracy, precision, and recall, creating a clinically applicable model for early bone cancer diagnosis and contributing to medical image analysis by combining hybrid optimization and deep learning techniques. The CNN will serve as the primary model for image classification, while Cuckoo Search Optimization will enhance feature selection and hyperparameter tuning. **Results:** CS-MHC ResNet demonstrated superior performance over other models in classification accuracy (above 90%), sensitivity (around 85%), precision (above 88%), and F-measure (approximately 86%). Other models (VGG-16, Xception, Inception) showed lower performance, indicating that the integration of CSO with ResNet enhances feature selection and improves the method's ability to classify bone cancer more effectively. These outcomes indicate that the proposed CS-MHC ResNet method offers significant improvements in the automated detection of bone cancer, supporting its potential for clinical use in diagnostic systems. **Conclusion:** The CS-MHC ResNet model combines Cuckoo Search Optimization (CSO) with ResNet for automated bone cancer detection. The model outperformed traditional deep learning architectures like VGG-16, Xception, and Inception in accuracy, sensitivity, precision, and F-measure. Key findings include enhanced model performance, improved feature selection via CSO, and faster convergence. The CS-MHC ResNet model shows promise for clinical applications, offering a more efficient and reliable tool for bone cancer detection. Future research will concentrate on larger multi-center datasets and simpler designs to improve resilience and applicability.

Keywords: Machine learning (ML)- Deep learning (DL)- Support vector machines (SVM)- Ant Colony Optimization

Asian Pac J Cancer Prev, **27 (3)**, 839-850

Introduction

According to the American Cancer Society, there will be about 3,970 new cases of primary bone and joint cancer in 2024 (2,270 in men and 1,700 in women), along with about 2,050 deaths (1,100 in men and 950 in women). These numbers include both adults and children. Less than 1% of all cancers are primary bone cancers, which start in the bones. Primary bone cancer is far less common in adults than bone metastasis cancer, which spreads to the bones from other organs. High-grade bone cancer differs markedly from healthy tissue, growing and spreading much more rapidly. These tumors are often classified as poorly differentiated. Early detection plays an essential role in developing survival outcomes for cancer patients.

The unique properties of malignant tissues make it difficult to detect and identify bone cancer using MRI and X-rays. Manual detection takes time, requires skill, and is

*[1]Department of Electronics and Communication Engineering, Jawaharlal Nehru Technological University, Kakinada, Andhra Pradesh, India. [2]Department of Electronics and Communication Engineering, Jawaharlal Nehru Technological University, Kakinada,Andhra Pradesh, India. *For Correspondence: mohanangel419@gmail.com*

prone to errors, particularly when dealing with small or complex tumors. By finding small similarities in images, machine learning (ML) can make diagnoses faster and more accurate. DL, a subset of ML, is particularly effective in tumor classification since it automatically extracts information. Traditional approaches, such as SVM and Edge Detection, while useful, frequently lack accuracy and generalizability, especially in early-stage cancer detection.

In recent years, a range of treatments for this condition have been explored, such as chemotherapy, surgery, radiation therapy, and targeted therapies. However, detecting cancer in bone tissue remains a challenging task due to its intricate nature. [1] Manual analysis of cancerous images is expensive, requiring specialized equipment, and may occasionally result in inaccurate conclusions due to mismanagement of details. Machine learning (ML) has become increasingly prevalent in cancer research, providing an efficient approach for data analysis and the automatic extraction of key information [2].

Preprocessing medical images is an essential step to develop the performance of ML models [3]. This process enhances image quality, allowing for more accurate data analysis. Common techniques used in image preprocessing include scaling, filtering, segmentation, pixel brightness adjustments, data augmentation, and normalization.

The way neurons in the human brain process information serves as the model for DL, a subset of ML. Artificial neurons, which are tiny units arranged in layers and connected to each other by weighted connections, are the fundamental building blocks of deep learning networks. Recently, the adoption of DL techniques has spurred progress across various fields, helping to address complex problems and improve the performance of existing research. Machine translation, sentiment analysis, speech recognition, image and face recognition, and signal processing are examples of DL applications [4].

Strong magnets and radio waves are used in magnetic resonance imaging (MRI) to produce finely detailed grayscale images. Image segmentation algorithms are capable of detecting abnormal bone growth in X-ray or MRI scans, helping to determine whether the growth is benign or malignant. Bone cancer diagnosis is based on factors such as the size, shape, and other characteristics of the growth. The process is typically divided into three stages: image processing, feature extraction, image segmentation, and classification.

Suganeshwari G and Balakumar R et al. [5] discussed an advanced approach for diagnosing bone cancer, offering valuable insights into the field of medical technology. However, its limited ability to capture comprehensive structural information may impact classification accuracy. Deep learning models, such as VGG16, were known for their "black-box" nature, making it tough to understand how the model arrives at its predictions. In medical settings, where comprehending the rationale behind a diagnosis is essential, this lack of interpretability could be problematic.

Ong W and Zhu L et al. [6] highlighted the Machine learning techniques, particularly those leveraging radiomic features from MRI, have proven highly effective in distinguishing between malignant and benign bone lesions, demonstrating strong accuracy in differentiating various tumor types. Integrating machine learning algorithms into clinical practice for bone malignancies could reduce unnecessary specialist referrals and follow-ups, leading to cost savings and alleviating patient anxiety. Additionally, accurate AI models can help identify high-risk bone lesions that require biopsy, enhancing confidence in the decision-making process and minimizing the risks of unnecessary biopsies, misdiagnoses due to small sample sizes, and the challenges of incorporating ML into existing clinical workflows [6].

Mohanthi Kakarla and Dr.K.Padma Raju [7] highlighted that FDG uptake in bone lesions, commonly used in imaging, may cause false positives for malignancy. Conditions such as fractures, bony hyperplasia, trauma, and metabolic bone diseases can complicate the evaluation and lead to incorrect diagnoses. To support informed decision-making, ML algorithms need to be integrated with domain-specific knowledge and trained on data derived from a wide range of real-world scenarios.

Sushopti Gawade and Ashok Bhansali et al. [8] discussed the efficacy of models like ResNet101 was demonstrated by the detection of osteosarcoma, a type of cancer that mainly affects bones, using convolutional neural networks and supervised deep learning techniques. These models achieve high accuracy with relatively minimal training time compared to others. The discussion also provides insights into the osteosarcoma dataset, emphasizing its higher prevalence among individuals aged 10 to 25 and those over 60. However, training large DL models, particularly convolutional neural networks, demands substantial computational resources, such as high-performance GPUs and large memory capacity, which can be a challenge for smaller healthcare facilities or research institutions with limited resources.

Ashish Sharma and Dhirendra P et al. [9] discussed the creation of an automated system for bone cancer early detection. To differentiate between cancerous and healthy bone based on texture and pixel intensity, the system uses medical image processing techniques like feature extraction, preprocessing, edge detection, and machine learning algorithms. Despite being known for their high accuracy, machine learning models like Random Forest and SVM were frequently perceived as black box methods, making it challenging to comprehend how the model makes its predictions.

Dama Anand1 and Osamah Ibrahim Khalaf et al. [10] concentrated on diagnosing bone cancer using DL frameworks for feature extraction and classification from histopathological images. Their findings could significantly influence the development of computer-assisted tools for cancer prognosis in radiology, offering a more accurate and efficient approach to bone tumor detection. However, the study may have relied on a specific dataset or imaging modality, which could limit the broader applicability of the outcomes to other populations or types of bone tumors.

M. Saritha and B.B. Prakash developed Combining image processing techniques and ML models develops the efficiency and accuracy of ALL detection. Automated technologies can help haematologists by delivering quick

and reliable analysis, resulting in prompt and appropriate treatment for patients. The approach highlights the potential for merging image processing and artificial intelligence to improve diagnostic processes in medical practice [11].

Nicola Ritte and James Cooper developed a method that incorporates connected components and automatic threshold selection, as well as a unique modification of Dijkstra's shortest path algorithm that use a unique graph representation, to achieve effective border detection and cell identification. The effort intends to increase diagnostic accuracy and efficiency by automating blood analysis, potentially decreasing the need for manual blood slide examination, which is time-consuming and prone to human error [12].

Bhagyashri G Patil and Sanjeev N found that, while both thresholding and watershed segmentation have advantages, the decision between the two is determined by the specific properties of the medical pictures and the diagnostic task. Combining or merging these methods with other image processing methods may develop the accuracy of detecting lung cancer cells [13].

Haralick and K. Shanmugam et al. established a collection of easily calculable textural features based on gray-tone spatial relationships and shown their efficacy in a variety of image classification tasks. The study had high identification accuracies (89% for photomicrographs, 82% for aerial images, and 83% for satellite imagery). These findings demonstrate the textural features' broad relevance in a variety of image-classification applications [14].

Kennedy J and R. C. Eberhart underlined that their approach to swarm intelligence varies from others, notably in terms of application and ease of implementation. They suggest that swarm-intelligent systems were simple to program and do not require deep understanding of individual behaviors and interactions, which emerge from simple rules. The word "particle swarm" was chosen to reflect the original inspiration from natural phenomena such as bird flocks and fish schools, which evolved into optimization algorithms that resembled particle swarms [15].

Yang and Xin-She cuckoos' brood parasitism demonstrated an impressive evolutionary adaptation, whereas the notion of Lévy flights provides insight into the movement patterns of numerous animals, including humans, and has applications in optimization and search strategies [16].

L. Sivayamini and C. Venkatesh's approach attempts to give a more precise and efficient way for wound assessment by combining the strengths of region-growing and watershed segmentation techniques [17].

Srishti developed a unique metaheuristic technique for detecting exudate in diabetic retinopathy using the Cuckoo Search algorithm and multi-level thresholds. The method focuses on edge identification and has shown more accuracy than previous techniques like Otsu's and Kapur's approaches. The findings show that the computational approach could be used objectively to evaluate retinal disease states, thereby benefiting ophthalmology [18].

Xin-She Yang and Suash Deb presented how swarm intelligence algorithms, like Particle Swarm and Cuckoo Search Optimization, have proven to be extremely efficient in addressing a wide range of nonlinear optimization problems in a variety of scientific and engineering disciplines. Despite its practical effectiveness, some problems remain that require additional investigation [19].

Abdesslem Layeb and Seriel Rayene Boussalia developed a novel stochastic technique according to the Quantum Inspired Cuckoo Search Algorithm (QICSA) to overcome the issue. They highlight two key contributions of their approach: the incorporation of a hybrid measure operation that includes the First Fit heuristic when the standard measure does not yield successful item packing, and the effective use of quantum representation to improve search efficiency [20].

H. Zheng, Y. and Zhou, A. presented a unique CSOA according to the Gauss distribution (GCS) to solve the constraints of the standard Cuckoo Search (CS) algorithm, particularly its slow convergence rate. When applied to standard test functions and engineering design optimization issues, the GCS method performs exceptionally well. GCS's optimal solutions outperform those obtained with the original CS algorithm [21]. The GCS method has a strong convergence rate, which reduces the number of generations required to find optimal solutions from 20.15 to 13.95.

Yang and Xin-She published the book "Cuckoo Search and Firefly Algorithm: Theory and Applications," which provides a complete introduction of nature-inspired algorithms, with a concentrate on the Cuckoo Search and Firefly Algorithm. These algorithms were popular due to their versatility, efficiency, and ease of implementation. The book digs into both theoretical and practical applications, providing thorough algorithm analysis, implementation instructions, and case study examples. Topics covered include multilevel image processing, feature selection, optimization challenges, and others. The resource was useful for scholars and practitioners in computer science, computational intelligence, and optimization [22].

Sathya R. and Abraham looked at two learning algorithms, supervised and unsupervised, to categorize postgraduate students based on their performance during the admissions period. Although the error back-propagation supervised learning technique is particularly effective for many non-linear real-time problems, we discovered that the unsupervised model outperforms the supervised learning approach in the case of student classification KSOM [23].

Ramkumar S and Malathi R. demonstrated high performance in classifying bone disorders, emphasizing the importance of combining statistical texture analysis with BMD measurements [24]. It could aid early detection of osteoporosis and osteopenia, particularly in resource-limited settings.

Ramkumar S and Kumar MR developed a precise and automated bone disorder classification system by estimating calcium concentration from radiological bone images using a binning technique and machine learning approach.A robust and accurate system capable of classifying bone disorders with 97.4% accuracy and 98.3% sensitivity.A validated model that provides a consistent

and automated diagnosis of bone health conditions[25].

Ramkumar S and Malathi study successfully integrates clinical and image-based analysis for improved bone disorder classification. The combination of medical data and machine learning enhances accuracy and reliability in diagnosis.The unique approach can help doctors make better clinical decisions for bone health assessment [26].

The aim of the study includes improving detection accuracy by merging Cuckoo Search Optimization (CSO) with ResNet for better picture classification. Optimizing model performance using CSO for better feature selection and faster convergence, Comparing the CS-MHC ResNet model to classic models like VGG-16, Inception, and Xception to enhance accuracy, precision, and recall, Developing a therapeutically relevant model for early bone cancer diagnosis Contributing to medical image analysis by using hybrid optimization and deep learning methods.

Materials and Methods

Dataset Description

The dataset for this study was created from radiological images obtained from the ION Diagnostics Centres in Chandapura and Bengaluru, comprising approximately 2,845 radiographic images representing five bone conditions: parosteal osteosarcoma, osteochondroma, enchondroma, Ewing sarcoma, and normal bone. These categories were selected for their diagnostic complexity, as each exhibits distinct growth patterns and radiographic characteristics.

To develop generalization, data augmentation methods like as rotation, flipping, contrast correction, Gaussian noise addition, and slight translation were used to increase the dataset to approximately 12,000 images while retaining essential diagnostic features such as calcification and cortical irregularity. Osteochondroma includes 2,480 images, Enchondroma 2,375, Parosteal Osteosarcoma 2,290, Normal Bone 2,165, and Ewing Sarcoma 2,090, for a moderately balanced dataset. Images were obtained using digital radiography (DR) and computed radiography (CR) equipment under defined protocols, with resolutions ranging from 512×512 to 1024×1024 pixels. To facilitate clinical correlation, each image was connected to anonymized patient details such as age, gender, and tumor site.

Ground truth labelling was performed by two board-certified radiologists and one pathology consultant, each with over ten years of experience, using a consensus-based review of radiological findings such as periosteal reaction, lesion margin, and calcification patterns, which were then verified against biopsy reports where available. The patients' average age was approximately 25.0 ± 5.5 years. The most commonly affected bones were the femur and tibia, which accounted for roughly 60% of cases.

Preprocessing

An input image used in Figure 1, which aims to integrate image segmentation with x-ray /CT/MRI technology for the treatment of cancer, a serious medical condition. The study evaluates various image segmentation techniques applied to x-ray or MRI data to detect abnormal bone growth patterns. It compares these techniques and suggests the most suitable method for different clinical scenarios.

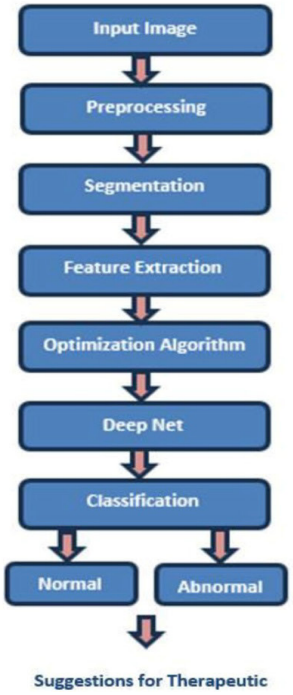

Figure 1. Methodology Flow Diagram to Achieve Output

Segmentation

The core objective of image segmentation is to divide an image into multiple regions or segments. Numerous empirical studies on diverse applications and techniques have been conducted by researchers in this crucial area of digital image processing research. A wide range of segmentation algorithms are available, but no single algorithm is universally effective for all types of images. Image processing applications require segmentation algorithms that deliver accurate results while minimizing processing time. This paper applies optimization algorithms to segment cancerous white blood cells (WBCs) from microscopic images [11-13]. Cuckoo Search Optimization (CSO) is the suggested algorithm, whereas Ant Colony Optimization (ACO) and Particle Swarm Optimization (PSO) are the current algorithms investigated.

Feature Extraction

Haralick et al. [14] presented a texture descriptor that works very well for describing texture characteristics. This descriptor computes particular pairs of pixel occurrences using each element (i, j) of the Gray Level Co-occurrence Matrix (GLCM) A. Four texture features contrast, correlation, energy, and homogeneity are calculated from the segmented image's grayscale values.

Contrast (Eq 1) measures the degree of local intensity variation in an image and is influenced by the distance between the maximum and minimum intensity levels.

$$CONT = \sum_{i,j} |i-j|^2 \boldsymbol{A}_{ij} \quad , \qquad (1)$$

Correlation (Eq 2) measures the extent to which pixels are spatially related or co-occurring throughout the entire image.

$$CORR = \sum_{i.j} \frac{(i-\mu_i)(j-\mu_j)\boldsymbol{A}_{ij}}{\sigma_i \sigma_j} \quad , \qquad (2)$$

here σ is denoted as the standard deviation and μ is indicated as the mean pixel value.

Energy (Eq 3) is controlled by the summation of squared parts.

$$E = \sum_{i,j} (\boldsymbol{A}_{ij})^2 \quad , \qquad (3)$$

Homogeneity

Homogeneity (Eq 4) quantifies the uniformity of the reduced-level distribution of regions; it is inversely based on the level of contrast.

$$H = \sum_{i.j} \frac{\boldsymbol{A}_{ij}}{1+|i-j|} \quad , \qquad (4)$$

Skewness

Skewness (Eq 5) assesses the degree of deviation from the standard distribution in an image. The range of pixel correlations is evaluated from -1 to +1.

$$SK = \sum \frac{((GLs-\mu_{GL})^3 * PixelCount)}{(NumberOfPixels-1)^3 * \sigma^3} \quad , \qquad (5)$$

Where μ indicated as the mean of y, σ is denoted as the standard deviation, and X(t) denotes the expected value of the quantity t. The skewness function is employed to compute the population value.

Skewness is determined not only by the amount of data points on either side of the mode, but also by their distance from it. In other words, a greater concentration of points on the left of the mode may not dominate over fewer points on the right if the latter are significantly farther away, resulting in a positive skewness even though more points are located on the left.

Variance (Eq 6) is defined as follows:

$$Var = \frac{1}{n} \sum_{i=1}^{n} |X_i - \mu|^2 \, , \qquad (6)$$

Where μ (Eq 7) is the mean of X:

$$\mu = \frac{1}{n} \sum_{i=1}^{n} X_i \, , \qquad (7)$$

Standard deviation

The standard deviation (Eq 8) is the square root of the variance defined as follows.

$$Std = \sqrt{\frac{1}{n} \sum_{i=1}^{n} |X_i - \mu|^2} \, , \qquad (8)$$

where μ (Eq 9) is the mean of X:

$$\mu = \frac{1}{n} \sum_{i=1}^{n} X_i \, , \qquad (9)$$

Entropy

Tumor segmentation in bone imaging is a highly challenging task. The normalized Shannon entropy (Eq 10&11) is employed for this segmentation process. Researchers have frequently employed Shannon entropy to tackle such complicated problems. The image is rotated by 35 degrees after being resized to 70 × 70 pixels based on different training and testing results.

$$E(X) = E(I(X)) = \sum_X p_y I(X) = -\sum_X p_y \, log_2 p_y \, , \qquad (10)$$

$$p_y = \frac{k_y}{m_1 . m_2}, \qquad (11)$$

Here ky represents the frequency of color x, and m_1 and m_2 denote the total number of rows and columns of the image, correspondingly. The intensity of cancerous bone regions is low, while the entropy of non-cancerous bone areas is high. To highlight this difference (Eq 12), the entropy is multiplied by the standard deviation.

$$D(X) = E(I(X)) = \sum_X p_y I(X) * \partial(X) = -\sum_X p_y \, log_2 p_y * \partial(X) \qquad (12)$$

Ant Colony Optimization (ACO)

ACO (Ant Colony Optimization) is a heuristic optimization technique used to address discrete optimization problems. It draws inspiration from ants' natural tendency to find the most effective routes between their nest and food sources [15]. As they look for food, ants leave pheromone trails, which other ants follow until they find the shortest route through the accumulated pheromone signals.

ACO algorithm

- Generate 'n' solutions randomly
- For individual ant A, select every variable for a selected value A=1,2,…m
- Evaluate objective function (Eq 13)
- Obtain good solution by changing the concentration of pheromone

$$p_{xy} = C \, p_{xy}(i-1) + \Delta \tau_{xy} \quad where \; i=1,2.....M \qquad (13)$$

Where, M denotes no. of iterations $p_{xy(i)}$ is the concentration of pheromone at i[th] iteration, p_{xy}*(i-1)* is the concentration of pheromone at (i-1)th iteration and C is denoted as pheromone evaporation rate, it's value ranges between 0 to 1. One drawback of ACO is that it takes longer to converge to an ideal solution in larger search spaces.

Particle Swarm Optimization (PSO)

Inspired by the social behavior of fish schools and flocks of birds, Drs. Eberhart and Kennedy introduced PSO (Particle Swarm Optimization), a population-driven stochastic optimization method, in 1995. Complex numerical maximization and minimization problems can

have their approximate solutions found using PSO. It can be applied to a variety of optimization tasks and is easy to implement. In this algorithm, when a particle moves from one position to another, it compares whether the previous position or the current one is closer to the goal, while also considering the information from neighboring particles [16].

Algorithm

• Initialize the particle with random motion & velocity vector
• Evaluate fitness *P*
• If P better than the P_{best}
• Set finest value of P_{best} as G_{best}
• Update velocity and position of particle
• Stop: giving G_{best} (optimal solution)

The velocity updates equation (Eq 14)

$$D(X)=E(I(X))= v$$

$$V_j\,(i+1) = V_j\,(i) + r_i(p_i(t) - Y_i(t) + ar_2(s(t) - Y_i(t) \quad (14)$$

Where w is called inertial weight and ranges between 0 to 1.

A drawback of PSO is that it typically requires more computational time compared to mathematical approaches.

Cuckoo Search Optimization (CSO)

In 2009, scientists Yang and Deb introduced the CSOA, which was inspired by the obligate brood parasitism behaviour of cuckoo species. Cuckoos lay their eggs in the nests of host birds, and the algorithm is according to three main rules [17, 18]:

1. Each cuckoo lays one egg at a time and randomly places it in a host bird's nest.

2. The nests that contain the highest-quality eggs are carried forward to the next generation.

3. In a fixed value of available nests, the host bird may discover an alien egg with a probability. Upon discovery, the host can either discard the egg or build a new nest.

Algorithm steps

1. Create n host nest first population.

2. Lay the egg (ap^1,bp^1) in p nest

Where ap^1=*ap+random walk (Levy flight)ap* (15)
bp^1=*bp+random walk (Levy flight)bp* (16)

3. Collate Cuckoo's egg fitness with the host egg fitness

4. If fitness of Cuckoo's egg is superior to host egg, swap the egg by Cuckoo's egg in p nest

5. If it finds the host bird then nest is discarded and fresh one is constructed.

Iterate step 2 to 5 up to criteria of termination is fulfilled [19-22].

Proposed Cuckoo Search with Modified Hill Climbing (CS-MHC)

The Cuckoo Search-Modified Hill Climbing (CS-MHC) [27] algorithm, as suggested, combines the global search ability of CSO with the local search capability of Stochastic Hill Climbing (HC). The main purpose of this integration is to accelerate convergence and avoid premature stagnation in the optimization process. In the standard CSO, new candidate solutions (eggs) are created by Levy flights, which is a means for global search. However, this could result in slow convergence when the population is near the optimal region. The proposed CS-MHC thus inserts a Hill Climbing operation just after the Levy flight update to get local assistance in overcoming this limitation. The hybridization enables the algorithm to achieve a better balance between exploitation and exploration. The change is in the solution update stage of CSO, where the newly generated Cuckoo solutions are first subjected to a local Hill Climbing search to get improved before fitness evaluation and nest replacement. This coupling leads to not only better accuracy but also the stability of the optimization process.

Algorithm steps

1. Create n host nest first population.
Each nest n contains a solution represented as (ap^1,bp^1)

2. Lay the egg (ap^1,bp^1) in p nest
Where ap^1=*ap+random walk (Levy flight)ap* (17)
bp^1=*bp+random walk (Levy flight)bp* (18)
This introduces global exploration capability

3. Collate Cuckoo's egg fitness with the host egg fitness

4. Apply Hill climbing as a local search on each new solution
Set Current_Position=(ap^1,bp^1)
Randomly select a Neighbor solution by slightly changing parameters in small steps.
If the neighbors' fitness is better or equal to the current position, update the current position.
Repeat until no better neighbors are found

5. Compare Fitness
If the hill-climbed cuckoo's eggs fitness is better than the host egg, replace the host egg with new one

6. A fraction of p_n of the worst nests are abandoned and replaced with new arbitrary solutions.

7. Rank all nests and identify the current best solution.

8. Repeat all nests and identify the present best solution.

Classification

Image classification is the process of assigning labels to specific groups of pixels based on defined criteria. In medical imaging, classification is primarily used to segment images into distinct regions, helping medical professionals in diagnosing and treating diseases. This process typically involves two steps: extracting features from the input image and analysing these features to categorize the dataset into specific classes.

Image classification can be categorized into two types

[23]: supervised, which uses features derived from a training set to classify input images (where target labels are known), and unsupervised, which automatically identifies specific classes without user intervention (where target labels are unknown), relying on the information within the algorithms [56]. Figure illustrates the various image classification approaches used to detect bone cancer.

In this study, ResNet-50 [28] architecture is utilized for supervised image classification to effectively extract deep hierarchical features from medical images, enabling accurate detection and categorization of bone cancer defects. Figure illustrates the various image classification methods used to detect bone cancer.

Results

This part describes the experimental outcomes and performance analysis of the suggested framework. The studies were carried out in a Google Colaboratory setting running Ubuntu 18.04/20.04 with Python 3.10 on an Intel® Xeon® CPU and 12.7 GB of RAM. To ensure fair and consistent model evaluation, the curated bone tumor dataset of 12,000 radiographic images representing five entities such as Parosteal Osteosarcoma, Osteochondroma, Enchondroma, Ewing Sarcoma, and Normal Bone was divided into three groups: 15% for validation, 70% for training, and 15% for testing. To improve generalization, data augmentation techniques such rotation (±35°), horizontal and vertical flipping, contrast modification, Gaussian noise addition, and slight translation were used. The model used a pre-trained ResNet-50 architecture on ImageNet, with the final layer updated to classify five bone tumor types. The CS-MHC technique was used to optimize model parameters, which combines Cuckoo Search's global exploration capacity with Hill Climbing's local refinement to achieve faster and more stable convergence. The main parameters employed were a batch size of 25, an initial learning rate of 0.0001, 26 epochs, a population size of 50, a maximum of 100 iterations, and a Levy flight exponent of 1.5. The proposed CS-MHC-based ResNet framework was tested against existing models to determine classification accuracy and robustness.

Sensitivity Analysis

From Table 1 and Figure 2, it is evident that the CS-MHC ResNet method outperforms other models in terms of sensitivity, which measures the method's ability to correctly identify cancerous bone tissue. The CS-MHC ResNet shows an average sensitivity increase of 6.06% compared to VGG-16, 5.01% compared to Xception, and 3.73% compared to Inception. This improved sensitivity indicates that the Cuckoo Search Optimization-based approach is more adept at detecting malignant lesions in bone scans, enhancing early diagnosis and treatment

Table 1. Average Sensitivity of CS-MHC

Parosteal osteosarcoma	VGG-16	Xception	Inception	ResNet	Hill Climbing-ResNet	Modified Hill climbing ResNet	CS-ResNet	CS-MHC ResNet
Osteochondroma	0.8711	0.8778	0.8933	0.9089	0.9111	0.9156	0.9178	0.92
Enchondroma	0.8655	0.88	0.8909	0.9273	0.9291	0.9291	0.9309	0.9327
Ewing sarcoma	0.8655	0.8745	0.8909	0.9036	0.9073	0.9091	0.9127	0.9182
Sensitivity - Blight	0.8125	0.825	0.835	0.8625	0.8675	0.8725	0.875	0.8825
Sensitivity - Normal	0.92	0.9233	0.9267	0.9378	0.9411	0.9433	0.9444	0.9522
Sensitivity - Average	0.86692	0.87612	0.88736	0.90802	0.91122	0.91392	0.91616	0.92112

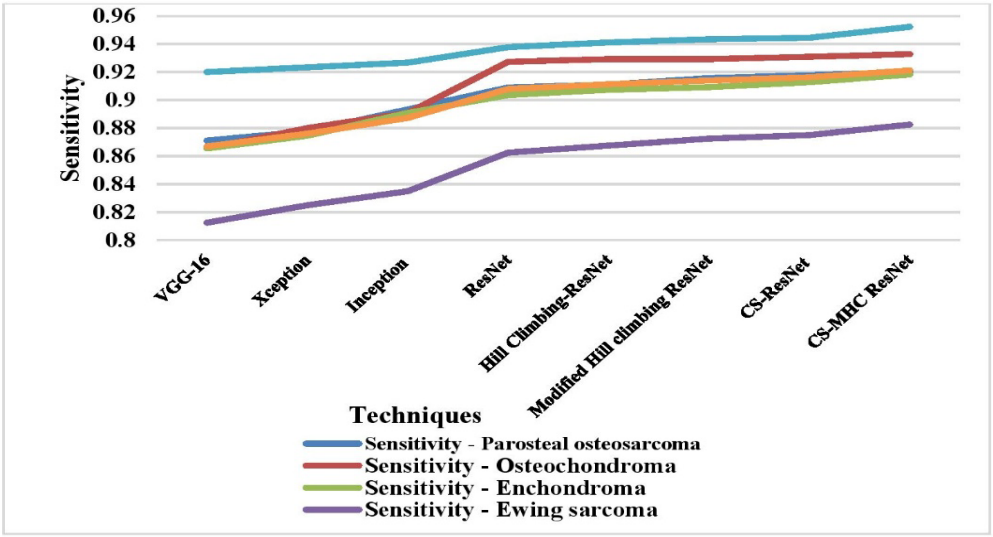

Figure 2. Average Sensitivity Measure for VGG-16, Xception, Inception,ResNet, Hill Climbing-ResNet ,Modified Hill Climbing ResNet, CS-ResNet and CS-MHC ResNet.

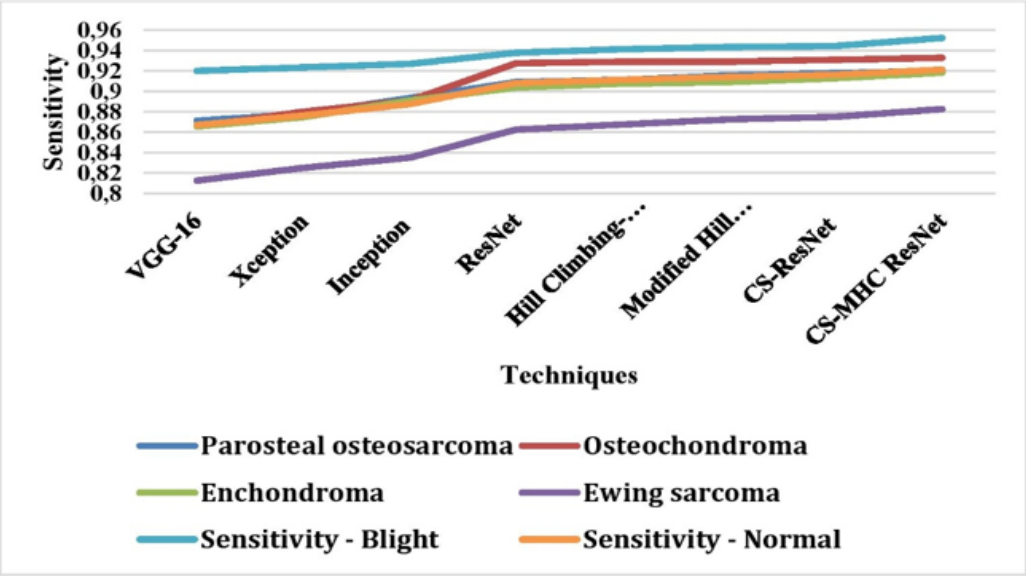

Figure 3. Average Precision of CS-MHC

Table 2. Average Precision of CS-MHC

	VGG-16	Xception	Inception	ResNet	Hill Climbing-ResNet	Modified Hill climbing ResNet	CS-ResNet	CS-MHC ResNet
Parosteal osteosarcoma	0.8467	0.8531	0.8683	0.8872	0.8913	0.8957	0.8959	0.9079
Osteochondroma	0.8546	0.8705	0.8845	0.9043	0.9076	0.9109	0.9159	0.9277
Enchondroma	0.853	0.8605	0.8734	0.9136	0.9156	0.9191	0.9194	0.9199
Ewing sarcoma	0.8486	0.8639	0.8675	0.8846	0.892	0.8949	0.8997	0.9028
Sensitivity - Blight	0.9314	0.9337	0.9402	0.9473	0.9485	0.9486	0.9497	0.9512
Sensitivity - Normal	0.86686	0.87634	0.88678	0.9074	0.911	0.91384	0.91612	0.9219

planning.

From the Figure 2 it can observed that the CS-MHC ResNet has higher Average Sensitivity by 6.06% of VGG-16, by 5.007% of Xception, by 3.73% of Inception, by 1.43% of ResNet, by 1.08% of Hill Climbing-ResNet, by 0.7847% of Modified Hill climbing ResNet, and 0.53% of CS-ResNet respectively.

Precision Analysis

As shown in Table 2 and Figure 3, the CS-MHC

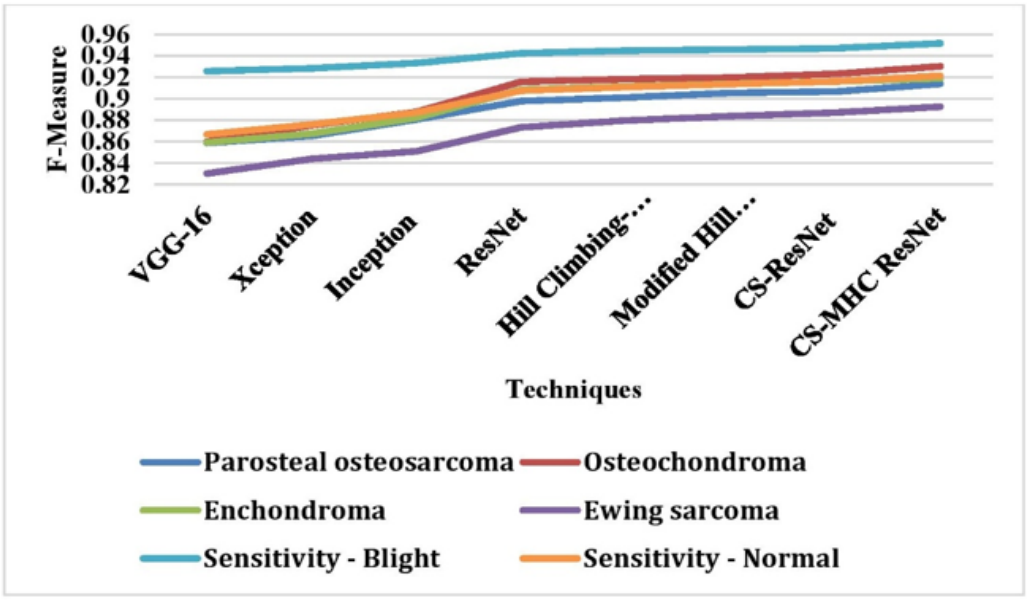

Figure 4. Average F-Measure of CS-MHC

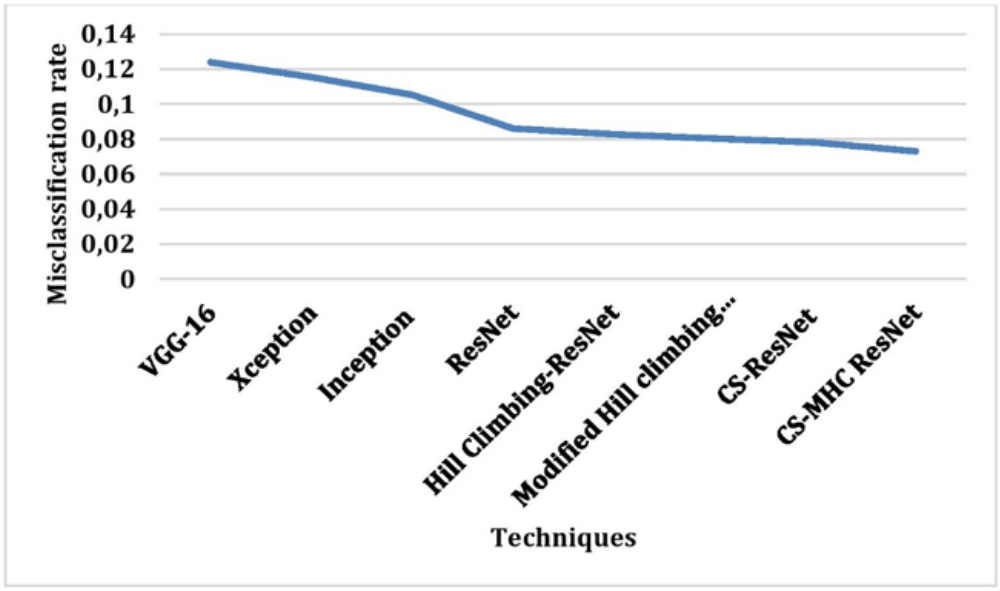

Figure 5. Average Misclassification Rate of CS-MHC

Table 3. Average F-Measure of CS-MHC

	VGG-16	Xception	Inception	ResNet	Hill Climbing-ResNet	Modified Hill climbing ResNet	CS-ResNet	CS-MHC ResNet
Parosteal osteosarcoma	0.8587	0.8653	0.8806	0.8979	0.9011	0.9055	0.9067	0.9139
Osteochondroma	0.86	0.8752	0.8877	0.9157	0.9182	0.9199	0.9233	0.9302
Enchondroma	0.8592	0.8674	0.8821	0.9086	0.9114	0.9141	0.916	0.919
Ewing sarcoma	0.8302	0.844	0.8509	0.8734	0.8796	0.8836	0.8872	0.8925
Sensitivity - Blight	0.9257	0.9285	0.9334	0.9425	0.9448	0.9459	0.947	0.9517
Sensitivity - Normal	0.86676	0.87608	0.88694	0.90762	0.91102	0.9138	0.91604	0.92146

Table 4. Average Misclassification Rate of CS-MHC

	VGG-16	Xception	Inception	ResNet	Hill Climbing-ResNet	Modified Hill climbing ResNet	CS-ResNet	CS-MHC ResNet
Misclassification Rate	0.1239	0.1154	0.1053	0.086	0.0828	0.0804	0.0782	0.073

ResNet also achieves a higher average precision score. Precision reflects the accuracy of the model in identifying positive instances (malignant lesions) without incorrectly labelling benign tissues. CS-MHC ResNet demonstrated a 6.15% improvement over VGG-16, a 5.06% improvement over Xception, and a 3.88% improvement over Inception. This improvement is crucial in minimizing false positives, which could lead to unnecessary treatments and biopsies for patients.

From the Figure 3 it can observed that the CS-MHC ResNet has higher Average Precision by 6.15% of VGG-16, by 5.06% of Xception, by 3.88% of Inception, by

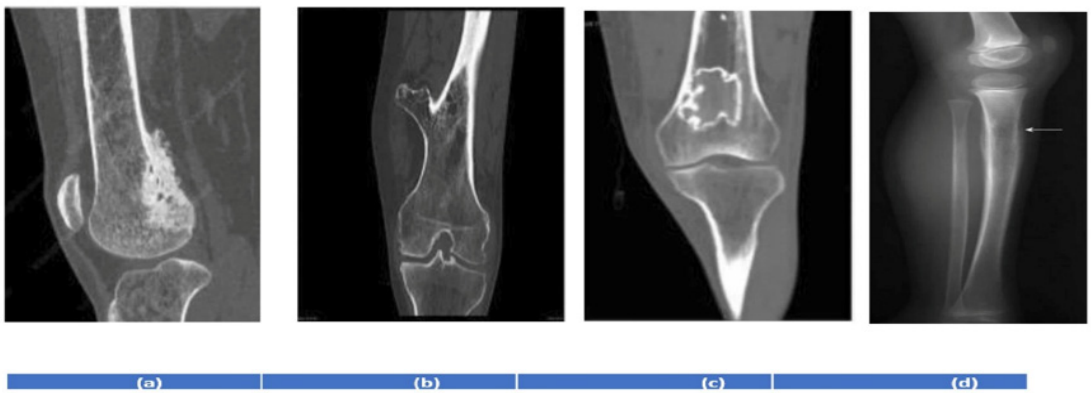

Figure 6. (a) Parosteal Osteosarcoma (b) Osteochondroma (c) Enchondroma (d) Ewing sarcoma

1.58% of ResNet, by 1.18% of Hill Climbing-ResNet, by 0.87% of Modified Hill climbing ResNet, and 0.62% of CS-ResNet respectively.

F-Measure Analysis

The F-Measure, which balances precision and recall, also favours the CS-MHC ResNet model, as seen in Table 3 and Figure 4. This metric is particularly valuable in clinical settings where both high sensitivity and high precision are essential to make sure the accuracy and reliability of diagnoses. CS-MHC ResNet shows an impressive performance with the highest F-Measure scores, confirming its robustness in distinguishing between benign and malignant bone tissues effectively.

From the Figure 4 it can observed that the CS-MHC ResNet has higher Average F-Measure by 6.11% of VGG-16, by 5.04% of Xception, by 3.81% of Inception, by 1.51% of ResNet, by 1.13% of Hill Climbing-ResNet, by 0.84% of Modified Hill climbing ResNet, and 0.58% of CS-ResNet respectively. Figure 5 it is observed that the Average Misclassification Rate of CS-MHC.

Discussion

The discussion surrounding bone tumors like parosteal osteosarcoma (POS), osteochondroma, enchondroma, and Ewing sarcoma is important due to their distinct characteristics, growth patterns, and diagnostic challenges. Parosteal osteosarcoma is a rare, slow-growing malignant tumor that typically arises on the surface of the bone. A 31-year-old lady develops osteosarcoma of the proximal tibial metaphysis following chemotherapy. The radiograph demonstrates that the periphery of the lesion has calcified following therapy and may be mistaken (Figure 6(a)).

Osteochondroma is the most common noncancerous bone growth, characterized by an overgrowth of both bone and cartilage, most commonly near the growth plate of long bones like the femur, tibia, or humerus. A 24-year-old lady with anterior knee discomfort caused by patellofemoral disease developed incidental enchondromas in the distal femoral diaphysis (Figure 6(b)).

Another kind of benign bone tumor that starts in the cartilage is called a chondroma. The flexible connective tissue that forms the majority of bones is called cartilage. Enchondroma are typically found in the small bones of the hands and feet, although they can appear in other bones as well. A 24-year-old lady with anterior knee discomfort caused by patellofemoral disease developed incidental enchondroma in the distal femoral diaphysis (Figure 6(c)).

Ewing sarcoma is a malignant tumor that arises from bone or soft tissue, often in the long bones or pelvis. It typically affects children and young adults and can be aggressive, requiring prompt treatment. In December 2011, a 20-year-old male college student in good health presented to his primary care physician with minor left knee soreness. A left knee radiograph was taken in May 2012, five months after his first presentation, and revealed a slight uneven lucency in the left medial femoral condyle (Figure 6(d)).

The radiological images (Figure 6(a)-(d)) sourced from ION Diagnostics Centre, Chandapura and Bengaluru. Each of these conditions presents unique diagnostic and therapeutic challenges. While some are benign and require minimal intervention, others, like Parosteal Osteosarcoma (POS) and Ewing Sarcoma, are malignant and demand more aggressive treatment. Advances in imaging, genetic testing, and molecular diagnostics are essential for distinguishing between these conditions, ensuring accurate diagnosis, and improving patient outcomes.

The experiments in this study provide valuable insights into the performance of ML approaches for detecting and classifying bone cancer from medical imaging data. This work focuses on advanced image processing techniques, including feature extraction, pre-processing, edge detection, and classification utilizing DL algorithms. It highlights the distinct texture differences between cancerous and healthy bone regions, where cancerous pixels exhibit irregular and scattered intensity patterns. Selecting appropriate texture and structural features is therefore crucial for accurate differentiation and diagnosis.

The study also addresses the limitations of traditional classification methods, emphasizing the role of precise image segmentation in identifying abnormal bone growth patterns. Additionally, Shannon entropy is utilized for image classification to enhance diagnostic reliability. The outcomes of the proposed CS-MHC ResNet method are compared with existing methods, including VGG-16, Xception, Inception, ResNet, Hill Climbing-ResNet, and Modified Hill Climbing ResNet, demonstrating superior performance across sensitivity, precision, and F-measure metrics.

The results show that the CS-MHC ResNet framework outperforms standard CNN-based models. It achieves an average sensitivity improvement of 6.06%, an average precision gain of 6.15%, and an F-measure rise of 6.11% over baseline models like VGG-16, Xception, and Inception. These upgrades demonstrate the model's enhanced capability for feature extraction and classification accuracy in medical imaging applications. In practical clinical applications, this enhancement leads to earlier tumor detection, fewer diagnostic errors, and lower patient risk, allowing radiologists to make faster and more reliable diagnostic decisions.

While the suggested performs well, it does have significant drawbacks. The dataset, although expanded, is very small and hospital-specific, which may limit generalizability. The combination of method creates high computational demands. Rare tumor types are underrepresented, which could influence classification accuracy. Future research will concentrate on larger multi-center datasets and simpler designs to improve resilience and applicability.

Author Contribution Statement

Mohanthi. K planned and carried out the simulations. Developed the theory and performed the computations. Contributed to the interpretation of the results. Dr. K Padmaraju has conceived of the given idea and supervised the findings of this work. All authors discussed the outcomes and contributed to the final manuscript.

Acknowledgements

General

We would like to sincerely thank everyone who helped make this research a success. First and foremost, we acknowledge the invaluable support and guidance of Dr.K Padma Raju, whose expertise and insights helped shape the direction of this work. We also extend our thanks to the research team for their collaborative efforts in implementing and testing the algorithms discussed in this study. We are particularly grateful to the developers of the CSOA, whose work has been instrumental in improving our approach. Our gratitude also goes to the creators of the various deep learning and machine learning frameworks that enabled us to experiment and enhance the performance of our detection and classification system.

Data Availability

The dataset analyzed during the present study is restricted due to patient privacy and institutional confidentiality policies. However, the data supporting the findings of this research are available from the corresponding author upon reasonable request and with the necessary institutional permissions

Conflict of Interest

The authors declare that they have no conflicts of interest related to the research given in this manuscript. The development of the automated system for detecting and classifying bone cancer was carried out independently, without any external financial or commercial support. No funding was received from any organization, and the results presented are solely based on the authors' own work and analysis.

References

1. Ranjitha MM, Taranath NL, Arpitha CN, CK S. Bone cancer detection using K-means segmentation and Knn classification. In2019 1st International Conference on Advances in Information Technology (ICAIT) 2019 Jul 25 (pp. 76-80). IEEE.
2. Eweje FR, Bao B, Wu J, Dalal D, Liao W, He Y, et al. Deep Learning for Classification of Bone Lesions on Routine MRI. EBioMedicine. 2021;68:103402. https://doi.org/10.1016/j.ebiom.2021.103402
3. Park CW, Oh SJ, Kim KS, Jang MC, Kim IS, Lee YK, et al. Artificial intelligence-based classification of bone tumors in the proximal femur on plain radiographs: system development and validation. PLoS One. 2022;17(2):e0264140. https://doi.org/10.1371/journal.pone.0264140..
4. Asri H, Mousannif H, Moatassime H, Noël T. Using machine learning algorithms for breast cancer risk prediction and diagnosis. Procedia Comput Sci. 2016 Dec 31;83:1064-9. https://doi.org/10.1016/j.procs.2016.04.224
5. Suganeshwari G, Balakumar R, Karuppanan K, Prathiba SB, Anbalagan S, Raja G. DTBV: a deep transfer-based bone cancer diagnosis system using VGG16 feature extraction. Diagnostics (Basel). 2023;13(4):757. https://doi.org/10.3390/diagnostics13040757
6. Ong W, Zhu L, Tan YL, Teo EC, Tan JH, Kumar N, et al. Application of machine learning for differentiating bone malignancy on imaging: a systematic review. Cancers (Basel). 2023;15(6):1837. https://doi.org/10.3390/cancers15061837
7. Kakarla M, Padma Raju K. Review of machine learning: views, architectures or techniques, challenges and future guidance, and real-world applications. Int Res J Adv Eng Manag (IRJAEM). 2024;2(3):545-51. https://doi.org/10.47392/IRJAEM.2024.0075
8. Gawade S, Bhansali A, Patil K, Shaikh D. Application of convolutional neural networks and supervised deep learning methods for osteosarcoma bone cancer detection. Healthc Anal. 2023;3:100153. https://doi.org/10.1016/j.health.2023.100153
9. Sharma A, Yadav DP, Garg H, Kumar M, Sharma B, Koundal D. Bone cancer detection using feature extraction based machine learning model. Comput Math Methods Med. 2021;2021:7433186. https://doi.org/10.1155/2021/7433186
10. Anand R, Khalaf O, Hajjej F, Wong S, Pan Y, Gogineni RC. Optimized swarm enabled deep learning technique for bone tumor detection using histopathological image. Sinergi. 2023;27:451-66. https://doi.org/10.22441/sinergi.2023.3.016
11. Saritha M. Detection of blood cancer in microscopic images of human blood samples. In: Proceedings of the International Conference on Electrical, Electronics and Optimization Techniques (ICEEOT); 2016 Mar 3–5; Chennai, India. Piscataway (NJ): IEEE; 2016. p. 596–600.
12. Ritter N, Cooper J. Segmentation and border identification of cells in images of peripheral blood smear slides. In: 30th Australasian Computer Science Conference (ACSC 2007), Conference in Research and Practice in Information Technology; 2007 Feb; Ballarat, Australia. Sydney (Australia): Australian Computer Society; 2007. p. 161–9.
13. Patil BG, Jain SN. Cancer cells detection using digital image processing methods. Int J Latest Trends Eng Technol. 2014;3:45-9.
14. Haralick RM, Shanmugam K, Dinstein I. Textural features for image classification. IEEE Trans Syst Man Cybern. 1973;SMC-3(6):610-21. https://doi.org/10.1109/TSMC.1973.4309314
15. Kennedy J, Eberhart RC, Shi Y. Swarm Intelligence, 1st Morgan Kaufmann. San Francisco, USA. 2001.
16. Yang XS, Deb S. Cuckoo search via Lévy flights. In: Proceedings of the World Congress on Nature and Biologically Inspired Computing (NaBIC); 2009 Dec 9-11; Coimbatore, India. Piscataway (NJ): IEEE; 2010. p.210-4.
17. Sivayamini L, Venkatesh C, Fahimuddin S, Thanusha N, Shaheer S, Sree PS. A novel optimization for detection of foot ulcers on infrared images. In2017 international conference on recent trends in electrical, electronics and computing technologies (ICRTEECT) 2017 Jul 30 (pp. 41-43). IEEE.
18. Srishti. Technique based on cuckoo search algorithm for exudates detection in diabetic retinopathy. Ophthalmol Res Int J. 2014;2(1):43-54.
19. Yang XS, Deb S. Cuckoo search: recent advances and applications. Neural Comput Appl. 2014;24:169-74. https://doi.org/10.1007/s00521-013-1367-1
20. Layeb A. A novel quantum inspired cuckoo search for knapsack problems. Int J Bio-Inspired Comput. 2011;3(5):297-305. https://doi.org/10.1504/IJBIC.2011.042260
21. Zheng H, Zhou Y. A novel cuckoo search optimization algorithm based on Gauss distribution. J Comput Inf Syst. 2012;8(10):4193-200.
22. Yang XS. Cuckoo search and firefly algorithm. 1st ed. Cham (Switzerland): Springer; 2014.22.
23. Sathya R, Abraham A. Comparison of supervised and unsupervised learning algorithms for pattern classification. Int J Adv Res Artif Intell. 2013;2(2):34-8. https://doi.

org/10.14569/IJARAI.2013.020206
24. Ramkumar S, Malathi R. Automatic bone disorder classification using hybrid texture feature extraction with bone mineral density. Asian Pac J Cancer Prev. 2018;19(11):3517-23. https://doi.org/10.31557/APJCP.2018.19.12.3517
25. Ramkumar S, Kumar MR, Sasi G. Programmed automatic bone disorder clustering based on cumulative calcium prediction for feature extraction. Clin Lab. 2022;68(8). https://doi.org/10.7754/Clin.Lab.2021.210844.
26. Ramkumar S, Malathi R. Clustering of various parameters to catalog human bone disorders through soft computing simulation. In: International Conference on ISMAC in Computational Vision and Bio-Engineering; 2018 May; Palladam, India. Cham (Switzerland): Springer International Publishing; 2019. p.1077-88.
27. Emambocus BAS, Jasser MB, Amphawan A. An optimized continuous dragonfly algorithm using hill climbing local search to tackle the low exploitation problem. IEEE Access. 2022;10:95030-45. https://doi.org/10.1109/ACCESS.2022.3204752
28. Younis A, Li Q, Afzal Z, Adamu MJ, Kawuwa HB, Hussain F, Hussain H. Abnormal brain tumors classification using ResNet50 and its comprehensive evaluation. IEEE Access. 2024;12:78843-53. https://doi.org/10.1109/ACCESS.2024.3403902